JOURNAL OF THERMOPHYSICS AND HEAT TRANSFER
Vol. 9, No. 2, April–June 1995

Unsteady Three-Dimensional Mixed Convective Airflow over a Horizontal Plate

C. C. Huang* and T. F. Lin†
National Chiao Tung University, Hsinchu 300, Taiwan, Republic of China

The buoyancy-induced longitudinal vortex rolls and the associated heat transfer in a mixed convective airflow over a horizontal heated plate were numerically investigated by directly solving the unsteady three-dimensional Navier-Stokes equations and the energy equation. Numerical results for the onset of vortex instability, the subsequent evolution of the longitudinal vortices, and the effects of these vortices on the heat transfer were carefully examined. The results indicate that steady two-dimensional laminar forced convection dominates for $Gr_z/Re_z^{1.5} < 100$. In the range of $Gr_z/Re_z^{1.5}$ from 100 to 200, three-dimensional vortex flow appears, accompanied with significant heat transfer enhancement. The vortex flow eventually reaches steady state when $Gr_z/Re_z^{1.5} < 300$. At a higher $Gr_z/Re_z^{1.5}$ the merging of the vortex rolls is seen and the resulting flow is unstable. With $Gr_z/Re_z^{1.5} > 600$ the vortex flow is relatively unstable. It was also noted that the parameter $Gr_z/Re_z^{1.5}$ is only appropriate for characterizing the heat transfer data. The detailed flow and thermal structures depend on both Re_z and Gr_z.

Nomenclature

A	=	aspect ratio, b/H
b	=	plate or channel width
Gr_H	=	Grashof number, $g\beta(T_w - T_e)H^3/\nu^2$
Gr_Z	=	local Grashof number, $g\beta(T_w - T_e)z^3/\nu^2$
Gr_Z^*	=	modified Grashof number for uniform wall heat flux
g	=	gravitational acceleration
H	=	channel height
h	=	local convection heat transfer coefficient
k	=	thermal conductivity
l	=	dimensional length of the heated plate
Nu	=	Nusselt number, hH/k
Nu_z	=	spanwise-average Nusselt number
P	=	dimensionless pressure, $p_m/\rho w_e^2$
Pr	=	Prandtl number, ν/α
p_m	=	dimensional dynamic pressures
Re_H	=	Reynolds number, w_eH/ν
Re_Z	=	Reynolds number, w_ez/ν
T, θ	=	dimensional and dimensionless temperatures, $(T - T_e)/(T_w - T_e)$
t, τ	=	dimensional and dimensionless time, $t/(H/W_e)$
U, V, W	=	dimensionless velocity components, u/w_e, v/w_e, and w/w_e
u, v, w	=	velocity components in x, y, z directions
X, Y, Z	=	dimensionless Cartesian coordinates, x/H, y/H, and z/H
x, y, z	=	Cartesian coordinates
α	=	thermal diffusivity
β	=	thermal expansion coefficient
ν	=	kinematic viscosity
ρ	=	density

Subscripts

e	=	values at the duct inlet
w	=	of wall quantities
z	=	based on the axial coordinate

Received March 21, 1994; presented as Paper 94-0206 at the AIAA/ASME 6th Joint Thermophysics and Heat Transfer Conference, Colorado Springs, CO, June 20–23, 1994; revision received Sept. 12, 1994; accepted for publication Sept. 21, 1994.

*Graduate Student, Department of Mechanical Engineering.
†Professor, Department of Mechanical Engineering.

Introduction

BUOYANCY resulting from temperature nonuniformity begins to significantly modify a forced flow and the associated heat transfer when its magnitude is comparable with the external force driving the flow. This flow modification is mainly affected by the relative orientation and magnitudes of the buoyancy and inertia forces, system geometry, method of heating (e.g., uniform wall temperature or heat flux), and the type of fluid. When the buoyancy is parallel with a forced flow as that in a vertical duct, it may reverse the flow direction, even in a buoyancy-aiding condition.[1] Apparently, this will cause a substantial change in the flow and thermal structures, and the flow may become unstable and transitional due to the presence of the inflection points in the velocity profiles. In a forced flow over a heated horizontal plate we often have a buoyancy normal to the flow direction. For an unstable heating configuration longitudinal and transverse vortices may be induced. In this horizontal flow the detailed characteristics of the steady and unsteady buoyancy-induced vortical flow are still not fully understood. This study intends to investigate the steady and unsteady secondary vortex flow in mixed convection over a heated horizontal plate through a transient three-dimensional numerical simulation.

Early studies on the mixed convective flow over a horizontal plate mainly focused on the situation in which the buoyancy is not high enough to cause flow separation, and hence, the flow is unidirectional and possesses a boundary-layer character. Solution methods based on similarity, local similarity, and nonsimilarity transformations were normally employed to analyze the problem. The effects of the buoyancy were frequently expressed in terms of local Nusselt number variations with a parameter formed from a certain combination of the local Reynolds and Grashof numbers.

Boundary-layer analysis of the buoyancy effects on the flow over a horizontal, isothermally heated plate was first carried out by Mori[2] and Sparrow and Minkowycz.[3] The flow equations were solved by expanding the solution into series around a perturbed parameter selected as $Gr_z/Re_z^{2.5}$. Sparrow and Minkowycz identified the conditions under which the buoyancy shows significant effects on the forced flow. The mixed convection parameter $Gr_z/Re_z^{2.5}$ was shown to be appropriate only for the Prandtl number of order of unity by Hieber.[4] Chen et al.[5] suggested that for $Gr_z/Re_z^{2.5} > 0.05$ or $Gr_z/Re_z^{2.5} < -0.03$, the airflow will be considerably affected by the buoyancy force. Similar analysis was performed by Mucoglu and Chen[6] for the plate subject to a constant heat flux. Sig-

nificant buoyancy effects occur for $Gr_z^*/Re_z^3 > 0.025$. Ramachandran et al.[7] extended their nonsimilarity related methods to cover the entire Prandtl number range and entire range of buoyancy forces from forced to natural convection.

A number of linear stability analyses have been reported in the literature to predict the onset of thermal instability. Wu and Cheng[8] assumed the disturbances in the form of stationary longitudinal vortices and used a nonparallel flow model. The proposed mixed convection parameter is $Gr_z/Re_z^{1.5}$. A similar vortex instability analysis was performed by Moutsoglou et al.[9] In their analysis the effects of buoyancy on the basic flow were included. Later, the dependence of the disturbances on the streamwise coordinate were considered by Yoo et al.[10] and Lee et al.[11-14] The predicted critical $Gr_z/Re_z^{1.5}$ is at least one order of magnitude below the experimental data. Chen and Chen[15] extended the above analysis to the Falkner-Skan flows. Experiments performed by Gilpin et al.[16] confirm the existence of the longitudinal vortices and provide the data for the onset of thermal instability on a horizontal Blasius flow of water heated from below. These longitudinal vortices were considered to be the first stage of the buoyancy-induced laminar-turbulent transition process in the flow. The detailed process of this buoyancy-induced flow transition was later experimentally examined by Imura et al.[17] They concluded that the onset of thermal instability occurs at a value of $Gr_z/Re_z^{1.5}$ approximately equal to 100. In the range of $Gr_z/Re_z^{1.5}$ from 100 to 300 the flow undergoes a transition from laminar forced convection to turbulent mixed convection. Additionally, their data for heat transfer coefficients indicate that $Gr_z/Re_z^{1.5}$ is a suitable mixed convection parameter. But Wang[18] experimentally shows that $Gr_z/Re_z^{2.2}$ is a suitable parameter. Similar experiments including flow visualization and detailed temperature and flow measurement from Takimoto et al.[19] and Moharreri et al.,[20] however, still suggest that $Gr_z/Re_z^{1.5}$ is an adequate parameter. The onset of instability for airflow was found to also be at $Gr_z/Re_z^{1.5} = 100$. Recently, Cheng et al.[21] moved further to examine the buoyancy effects in the transition regime ($2.5 \times 10^4 < Re_z \leq 2.2 \times 10^6$). $Gr_z/Re_z^{2.7}$ was found to be a good parameter for turbulent mixed convective horizontal flow.

The above literature review clearly indicates that the onset point is significantly underpredicted by the linear stability analysis. Although several detailed measurements have been carried out in the literature, the detailed characteristics of a mixed convection flow over a heated horizontal plate are still not well understood. For instance, the choice of a suitable mixed convection parameter solely based on the data of heat transfer coefficient needs to be re-examined. The present study intends to explore the detailed processes of the vortex formation and subsequent flow development in the mixed convective airflow over a horizontal flat plate through an unsteady three-dimensional numerical simulation.

Analysis

Mathematical Formulation

The physical system under consideration is mixed convection over an isothermally heated horizontal plate. Note that mixed convection in a bottom heated horizontal rectangular channel can approximate the mixed convection over a horizontal plate if the boundary-layer thickness on the plate is much smaller than the channel height. Instead of directly simulating the external mixed convective flow, which is relatively difficult numerically, we consider the situation in Fig. 1. An isothermal horizontal flow at T_e with a uniform inlet velocity w_e enters a horizontal rectangular channel. Initially, the flow in the entire channel is isothermal at T_e. At a certain instant of time, designated as time = 0, it is assumed that the bottom plate temperature is suddenly raised to a uniform value T_w over a finite length l, and is maintained at this level thereafter. Meanwhile, all other surfaces of the channel are

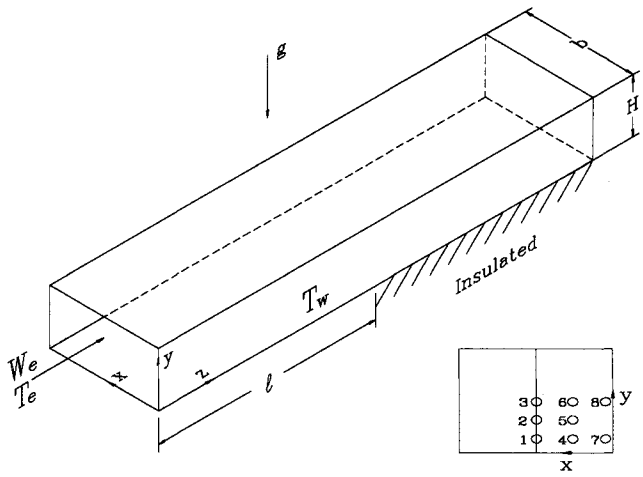

Fig. 1 Schematic of the physical model and the detection points, point 1—(0.5, 0.025), 2—(0.5, 0.057), 3—(0.5, 0.09), 4—(0.254, 0.025), 5—(0.254, 0.057), 6—(0.254, 0.09), 7—(0.041, 0.025), 8—(0.041, 0.09).

thermally well-insulated. Immediately after the elevation of the plate temperature, the fluid adjacent to the plate is heated and an upward buoyancy is generated, which displaces the flow to deviate from the horizontal direction. As the process continues, the buoyancy gets stronger and affects a larger region due to the diffusion and convection of heat by the flow. Hence, the flow can be significantly modified when the buoyancy is large compared to the inertia force. New flow structures may be induced in the flow. The flow can become oscillatory and transitional and is obviously three dimensional. The detailed processes of flow evolution from a simple unidirectional flow to a complex unsteady three-dimensional vortex flow will be numerically simulated.

The appropriate dimensionless flow equations with the Boussinesq approximation are

$$\frac{\partial U}{\partial X} + \frac{\partial V}{\partial Y} + \frac{\partial W}{\partial Z} = 0 \tag{1}$$

$$\frac{\partial U}{\partial \tau} + U\frac{\partial U}{\partial X} + V\frac{\partial U}{\partial Y} + W\frac{\partial U}{\partial Z} = -\frac{\partial P}{\partial X} + \frac{1}{Re_H}\left(\frac{\partial^2 U}{\partial X^2} + \frac{\partial^2 U}{\partial Y^2} + \frac{\partial^2 U}{\partial Z^2}\right) \tag{2}$$

$$\frac{\partial V}{\partial \tau} + U\frac{\partial V}{\partial X} + V\frac{\partial V}{\partial Y} + W\frac{\partial V}{\partial Z} = -\frac{\partial P}{\partial Y} + \frac{1}{Re_H}\left(\frac{\partial^2 V}{\partial X^2} + \frac{\partial^2 V}{\partial Y^2} + \frac{\partial^2 V}{\partial Z^2}\right) + \frac{Gr_H}{Re_H^2}\theta \tag{3}$$

$$\frac{\partial W}{\partial \tau} + U\frac{\partial W}{\partial X} + V\frac{\partial W}{\partial Y} + W\frac{\partial W}{\partial Z} = -\frac{\partial P}{\partial Z} + \frac{1}{Re_H}\left(\frac{\partial^2 W}{\partial X^2} + \frac{\partial^2 W}{\partial Y^2} + \frac{\partial^2 W}{\partial Z^2}\right) \tag{4}$$

$$\frac{\partial \theta}{\partial \tau} + U\frac{\partial \theta}{\partial X} + V\frac{\partial \theta}{\partial Y} + W\frac{\partial \theta}{\partial Z} = \frac{1}{Re_H Pr}\left(\frac{\partial^2 \theta}{\partial X^2} + \frac{\partial^2 \theta}{\partial Y^2} + \frac{\partial^2 \theta}{\partial Z^2}\right) \tag{5}$$

subject to the following initial and boundary conditions:

at $\tau = 0$

$U = V = 0$, W = steady isothermal flow in the duct (6)

at $\tau > 0$:

at $Z = 0$

$$U = V = W - 1 = \theta = 0 \tag{7}$$

at $Z = 2l/H$

$$\frac{\partial U}{\partial Z} = \frac{\partial V}{\partial Z} = \frac{\partial W}{\partial Z} = \frac{\partial \theta}{\partial Z} = 0 \tag{8}$$

at $Y = 0$ and $Z \leq l/H$

$$\theta - 1 = U = V = W = 0 \tag{9}$$

at all other surfaces

$$\frac{\partial \theta}{\partial n} = U = V = W = 0 \tag{10}$$

where n is a unit normal to a surface. The above equations were written in terms of the nondimensional variables defined in the nomenclature. Note that in the above formulation an insulated section of length l is added to the exit end of the heated section to facilitate the prescription of the outflow boundary conditions in the present elliptic flow analysis. This added section must be long enough so that the downstream boundary condition [Eq. (8)], is suitable.

The local Nusselt number on the heated plate is defined as

$$Nu = \frac{h \cdot H}{k} = -\left.\frac{\partial \theta}{\partial Y}\right|_{Y=0} \tag{11}$$

and the spanwise-averaged Nusselt number is defined as

$$Nu_z = \frac{1}{b}\int_0^b \frac{hz}{k}\,\mathrm{d}x = \frac{Z}{A}\int_0^A \left(-\left.\frac{\partial \theta}{\partial Y}\right|_{Y=0}\right)\mathrm{d}X \tag{12}$$

where A is the aspect ratio of the channel.

Solution Method

In view of the complex unsteady three-dimensional mixed convective vortex flow to be simulated, a highly efficient and accurate numerical scheme is needed. We chose the projection method[22] combined with the higher-order finite difference spatial discretization to solve the Navier-Stokes and energy equations in primitive form on a uniform, but staggered, grid system.

In discretizing the above equations, a third-order upwind scheme developed by Kawamura et al.[23] is employed to discretize the convective terms. Specifically, a typical convective term is approximated as

$$u\left.\frac{\partial f}{\partial x}\right|_i \approx u\,\frac{-f_{i+2} + 8f_{i+1} - 8f_{i-1} + f_{i-2}}{12\Delta x} + |u|\,\frac{f_{i+2} - 4f_{i+1} + 6f_i - 4f_{i-1} + f_{i-2}}{4\Delta x} \tag{13}$$

where f denotes the velocity components or temperature. The diffusive terms are approximated by a fourth-order central difference.[24] For instance

$$\frac{\partial^2 f}{\partial x^2} \approx (-f_{i+2} + 16f_{i+1} - 30f_i + 16f_{i-1} - f_{i-2})/12(\Delta x)^2 \tag{14}$$

Time advancement may be done either implicitly or explicitly. The first-order Euler explicit scheme was employed since it was easy to implement and requires much less computer memory allocation than any equivalent implicit implementation. The stability of the scheme is limited by the requirement that the Courant number be less than unity.[25] To insure the numerical convergence, the Courant number is set below 0.05 in the computation, which leads to

$$\Delta\tau < 0.05 \cdot \min\left(\frac{\Delta X}{U_{\max}}, \frac{\Delta Y}{V_{\max}}, \frac{\Delta Z}{W_{\max}}\right) \tag{15}$$

The above solution method is verified by comparing our prediction at large τ with the data reported by Moharreri et al.[20] for mixed convective airflow over an isothermal horizontal plate. Their experimental condition for the data chosen for comparison is $w_\infty = 34$ cm/s, $T_w - T_\infty = 30$°C, $b = 30$ cm, and $l = 104$ cm. By choosing $H = b$, the case corresponds to $Re_H = 6376$, $Gr_H/Re_H^2 = 2.63$, and $A = 1$. Note that the reason for choosing the height of the channel to be the same as its width is to insure the boundary-layer thickness over the entire heated plate to be much smaller than the channel height. Computation was performed by using a 61 × 61 × 41 grid. This comparison is shown in Fig. 2 for the spanwise variations of the axial velocity W and temperature θ at $z = 29.5$ cm and $y = 0.5$, 1.5, and 3.0 cm. The agreement is good. Our predicted temperature contours are also in good agreement with the incipience and growth of mushroom-type vortices visualized by Moharreri et al.[20] Furthermore, the predicted spanwise-average Nusselt number also agrees well with the data of Takimoto et al.[19] Finally, the grid-independence test is conducted. Sample results from such tests indicate that the oscillation frequency of the flow, a very important characteristic of the oscillatory flow, calculated from the 61 × 61 × 41, 71 × 71 × 41, and 71 × 81 × 51 grids for a typical case with $Re_H = 4000$ and $Gr/Re_H^2 = 3$ are, respectively, 0.210, 0.208, and 0.208. The differences between them are all less than 3%. Additionally, the spanwise-average Nusselt number predicted from these grids for the same case also shows good agreement. Good agreement is also noted for the time oscillation of W and θ at the sampling locations. Through these program tests, the adopted solution procedures are considered to be suitable for the present study.

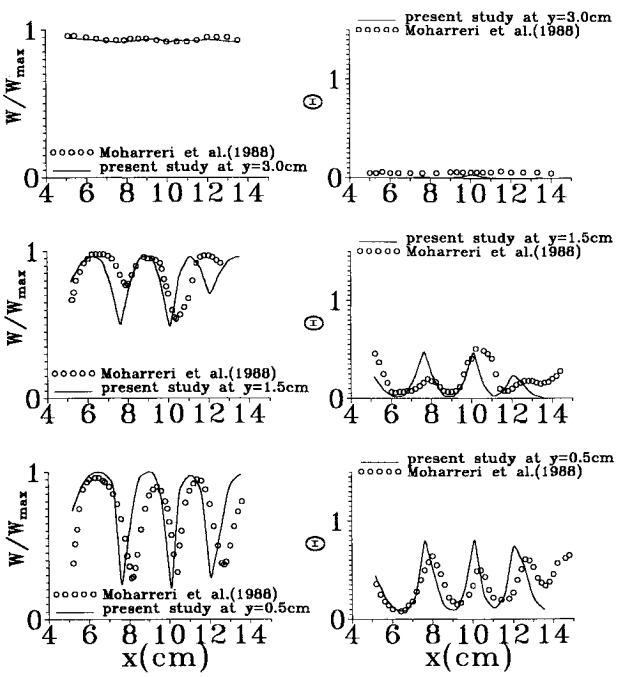

Fig. 2 Spanwise distributions of the streamwise velocity and temperature ($w_e = 34$ cm/s, $T_w - T_e = 30$°C, $z = 29.5$ cm, $y = 0.5$, 1.5, and 3.0 cm).

Results and Discussion

The foregoing problem formulation indicated that the problem under consideration is governed by five nondimensional parameters: 1) Pr, 2) Re_H, 3) ratio of buoyancy to inertia forces Gr_H/Re_H^2, 4) A, and 5) length of the heated section l/H. To simulate mixed convection of air over an isothermally heated horizontal plate, Pr is fixed at 0.7, A is taken to be unity, l/H is selected as 3.5, and Re_H is chosen to be above 3000 to insure the boundary-layer thickness on the heated plate to be much smaller than the channel height. The parameter Gr_H/Re_H^2 is chosen to insure the generation of the vortices, which is expected to occur when $Gr_Z/Re_Z^{1.5} > 100$. Based on this criterion, Gr_H/Re_H^2 is varied from 2 to 6. The predicted results for the cases specified by Re_H and Gr_H/Re_H^2 can be easily transformed to the parameters normally used in the mixed convective flow over a horizontal plate, namely, Re_Z and $Gr_Z/Re_Z^{1.5}$.

The results are first presented for a case with the convective stability parameter $Gr_Z/Re_Z^{1.5}$ not much larger than 100. For clear illustration of the formation of the vortices, the spatial distributions of the local Nusselt number on the heated bottom plate are shown in Fig. 3 for steady state for $Re_H = 4000$ and $Gr_H/Re_H^2 = 2$. At $\tau \geq 18.39$ steady state is already reached. The results reveal that in the entry portion at small Z (<0.9) the flow remains two dimensional and heat transfer is dominated by forced convection. Nu decreases with the downstream distance, indicating the entrance effects in the duct. At certain critical downstream distances depending on the spanwise location, longitudinal vortices are induced by the upward buoyancy. The critical distance is shorter near the side walls ($X = 0$ and 1). This means that the vortices are first induced in the bottom corners simply because heat is accumulated in these regions and the buoyancy is higher therein. For clarity, the critical Z is defined as the location at which the heat transfer coefficient is augmented by the vortices by 3% as compared to the forced convection value. This will become evident later. Six pairs of vortex rolls are clearly seen on the plate for $2.3 \leq Z \leq 2.8$. The vortices cause significant heat transfer enhancement over the pure forced convection. However, the one near the side wall disappears as the flow approaches the exit end, resulting in five pairs of vortices there.

To directly demonstrate the evolution of the vortices, the secondary flow and temperature distributions at various cross sections are examined. Since the flow was found to be symmetric with respect to the midplane $X = 0.5$, and the generated vortices were very close to the bottom wall in the computation, only the isotherms in the lower left quarter ($0 \leq X \leq 0.5$, $0 \leq Y \leq 0.5$) and cross plane streamlines for the lower right quarter ($0.5 \leq X \leq 1.0$, $0 \leq Y \leq 0.5$) of the channel are presented together in Fig. 4. These results clearly show the earlier appearance of the first pair of vortices near the side wall at the location where $Gr_Z/Re_Z^{1.5}$ is about 100. A second pair of vortices emerge in regions adjacent to the first one at $Gr_Z/Re_Z^{1.5} = 183.2$. At $Gr_Z/Re_Z^{1.5} = 442.4$, another pair of vortices near the midplane $X = 0.5$ appear. Comparison of the stream function values at various cross sections and times indicates that the secondary vortex flow becomes

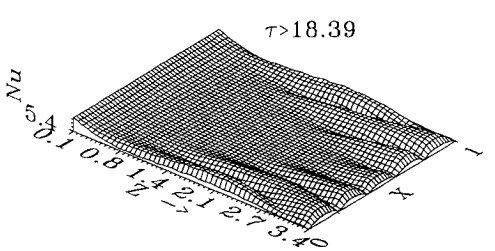

Fig. 3 Steady local Nusselt number distributions on the bottom plate for $Re_H = 4000$ and $Gr_H/Re_H^2 = 2$.

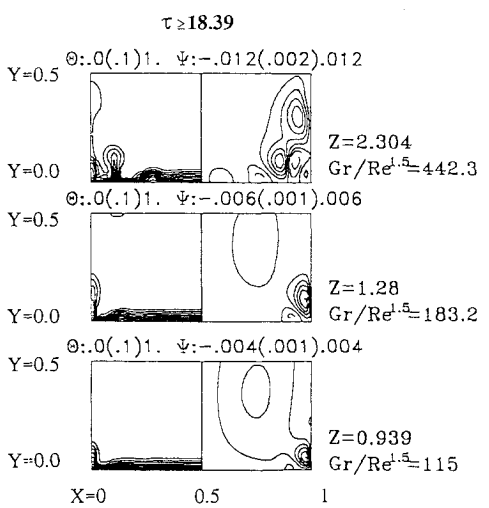

Fig. 4 Isotherms and streamlines for secondary flow at various cross sections at steady state for $Re_H = 4000$ and $Gr_H/Re_H^2 = 2$.

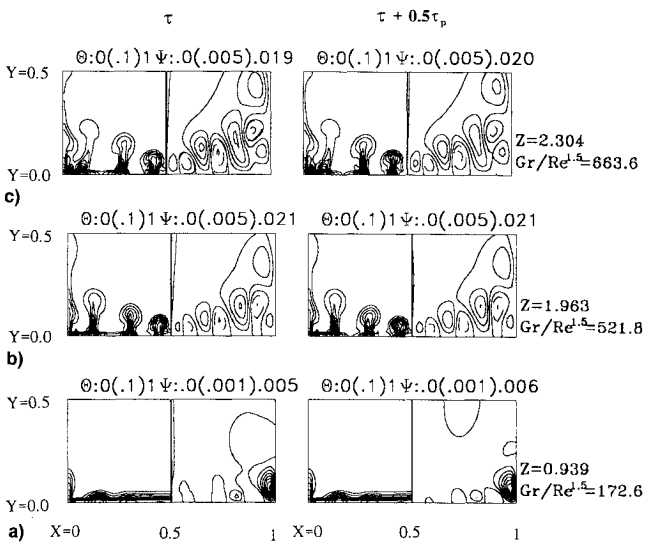

Fig. 5 Secondary flow in a typical period at a large τ for $Re_H = 4000$ and $Gr_H/Re_H^2 = 3$ at $Z =$ a) 1.0, b) 2.0, and c) 2.3. The period of the oscillation τ_p is about 5.1.

stronger with the downstream distance and with time. Although the flow eventually approaches steady state, the longitudinal vortex roll patterns are rather irregular.

Next, the effects of Gr_H/Re_H^2 are examined. The predicted local Nusselt number distributions for $Gr_H/Re_H^2 = 3$ and $Re_H = 4000$ indicate that at this higher buoyancy the flow becomes time periodic after the initial transient. It is noted that the longitudinal vortices appear earlier for a higher Gr_H/Re_H^2. For $Gr_H/Re_H^2 = 3$ the critical distance for the appearance of the vortex rolls is in the range $Z = 0.6$–0.7. This range is normally considered as the onset point of the vortex instability corresponding to the value of the mixed convection parameter $Gr_Z/Re_Z^{1.5}$, ranging from 88 to 111. This value again is in good agreement with the measurement of Gilpin et al.,[16] Imura et al.,[17] Takimoto et al.,[19] and Moharreri et al.[20] Note that the wavelength of the vortices varies from roll-to-roll, and it gradually increases in the flow direction. Finally, it is again noted that large heat transfer enhancement results due to the vortex flow. Examining the secondary flow shown in Fig. 5 for $Gr_H/Re_H^2 = 3$ reveals that at a higher value of Gr_H/Re_H^2 the secondary flow is stronger and the three-dimensional vortex flow does not approach steady state at large τ. Note that the cellular flow motion at the cross section $Z = 2.304$ (or $Gr_Z/Re_Z^{1.5} = 663.6$) is relatively irregular in space. The characteristics of this irregular flow can be obtained by checking

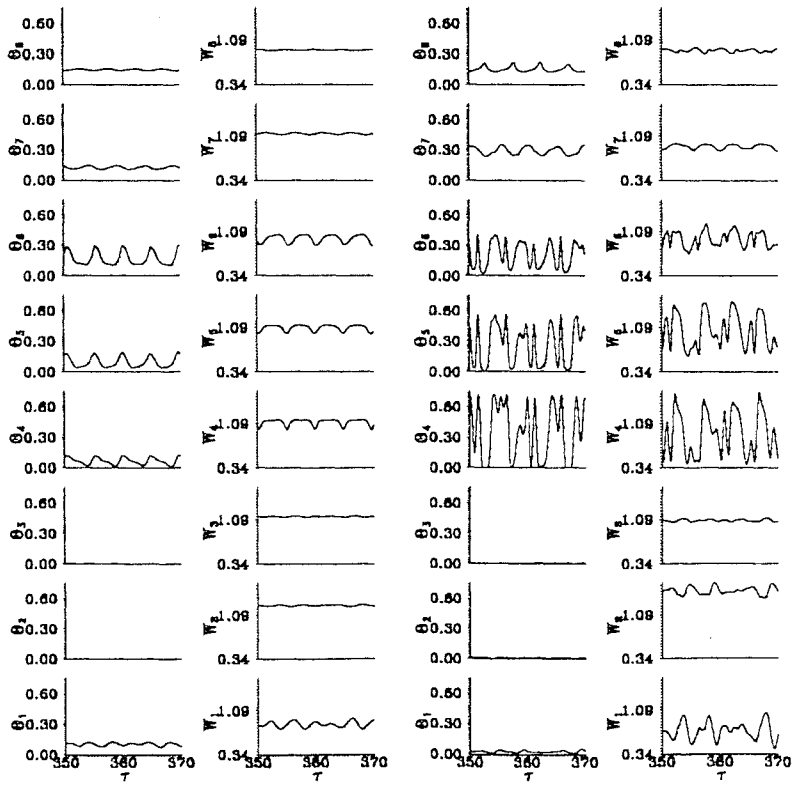

Fig. 6 Time histories of the axial velocity and temperature at Z = 1.963 and 3.329 at eight selected locations for Re_H = 4000 and Gr_H/Re_H^2 = 3.

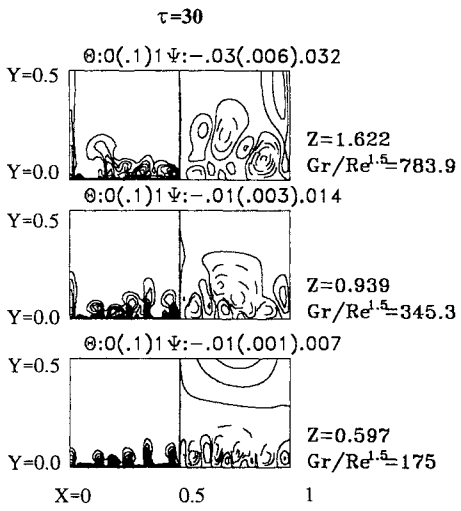

Fig. 7 Isotherms and streamlines for secondary flow at various cross sections at τ = 30 for Re_H = 4000 and Gr_H/Re_H^2 = 6.

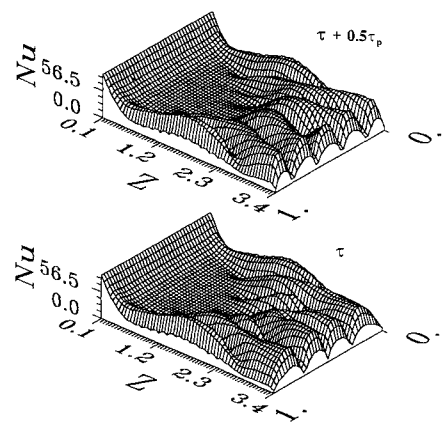

Fig. 8 Local Nusselt number distributions of the bottom plate in a typical period at a large τ for Re_H = 3000 and Gr_H/Re_H^2 = 3. The period of the oscillation τ_p is about 4.688.

with the time samples of W and θ given in Fig. 6 for selective locations. The coordinates of these detection points are specified in Fig. 1. It is noted that in the vortex flow the velocity and temperature oscillations intensify as the flow moves downstream, reflecting that the flow becomes increasingly unstable as it travels downstream. Near the leading edge the flow is essentially steady. At Z = 1.963 the flow is time periodic. Further downstream, large amplitude, irregular velocity, and temperature oscillations exist at several locations at the cross section Z = 3.329.

To further explore the unstable mixed convective vortex flow characteristics, results for higher buoyancy strength are examined. The isotherms and streamlines of the secondary flow at various cross sections at τ = 30 are presented in Fig. 7 for Gr_H/Re_H^2 = 6, with other parameters fixed. Contrasting these results with those for Gr_H/Re_H^2 = 3 in Fig. 5 again reveals that at a higher buoyancy the longitudinal vortices appear earlier and the critical downstream distance from the leading edge for the onset of the vortices are shorter. It is of interest to note that the vortices at various spanwise locations are almost simultaneously initiated at this high buoyancy. Also, more longitudinal rolls were induced, i.e., the wavelength of the vortex rolls is shorter. It is also important to note that the combination of the vortices into larger rolls takes place around Z = 1.0 ($Gr_Z/Re_Z^{1.5}$ = 380), which was also observed in the experiment of Moharreri et al.[20] The combined vortex rolls become rather irregular, apparently implying the oscillatory and unstable character of the flow. The time records of the velocity and temperature show that at Gr_H/Re_H^2 = 6 the fluc-

tuations in W and θ are much more intense and contain higher frequencies and are relatively unstable, reflecting that the flow could be in transition or turbulent regime.

Next, the effects of the Reynolds number are to be discussed. Figures 8 and 9 respectively present the local Nusselt number distributions on the bottom plate and the secondary flow and temperature fields at several cross sections in a typical period at large τ for a lower Reynolds number, Re_{II} = 3000 and Gr_{II}/Re_{II}^2 = 3. When these results are contrasted with those for Re_{II} = 4000 and Gr_{II}/Re_{II}^2 = 3 in Fig. 5, it is noted that the qualitative flow structures for these two Reynolds numbers are quite similar. But for Re = 3000, the flow is time periodic in the entire duct. A close inspection of the detailed flow and thermal structures, however, discloses that at lower Re_{II}, the rolls are slightly smaller. However, the flow oscillates in a lower frequency with larger amplitude (Fig. 10). Results for a higher buoyancy with Re_{II} = 3000 and Gr_{II}/Re_{II}^2 = 4 also show the merging of adjacent vortices in the downstream region. After the cell merging the flow is nonperiodic, and hence, highly unstable.

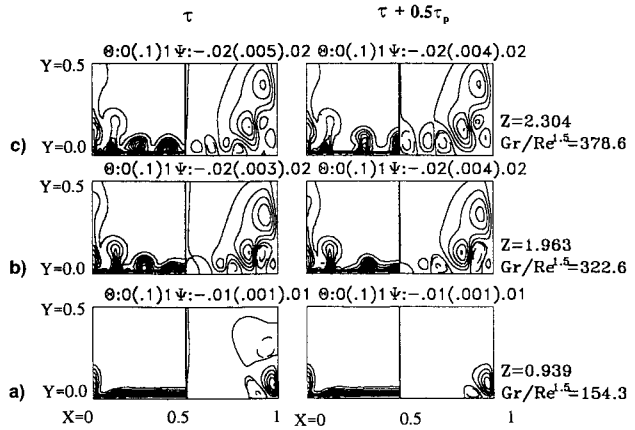

Fig. 9 Secondary flow in a typical period at a large τ for Re_H = 3000 and Gr_H/Re_H^2 = 3 at Z = a) 1.0, b) 2.0, and c) 2.3. The period of the oscillation τ_p is about 4.688.

Experimental data for heat transfer coefficient are often expressed in terms of $Nu_Z/Re_Z^{0.5}$ vs $Gr_Z/Re_Z^{1.5}$.[19,26] Our predicted results for various cases are shown in Fig. 11, which clearly show the heat transfer enhancement by the induced vortices for $Gr_Z/Re_Z^{1.5} \geq 100$. These data can be correlated by the equation:

$$Nu_Z/Re_Z^{0.5} = 0.003(Gr_Z/Re_Z^{1.5}) - 0.005, \text{ for } Gr_Z/Re_Z^{1.5} > 100 \quad (16)$$

Does the excellent fit of the experimental and numerical heat transfer data using the parameter $Gr_Z/Re_Z^{1.5}$ suggest that it is a suitable parameter for characterizing the mixed convection flow over the horizontal plate? This question can be answered by examining the flow and temperature fields at the same value of $Gr_Z/Re_Z^{1.5}$ from various cases presented above. A careful comparison of the results in Figs. 4, 5, and 7 clearly

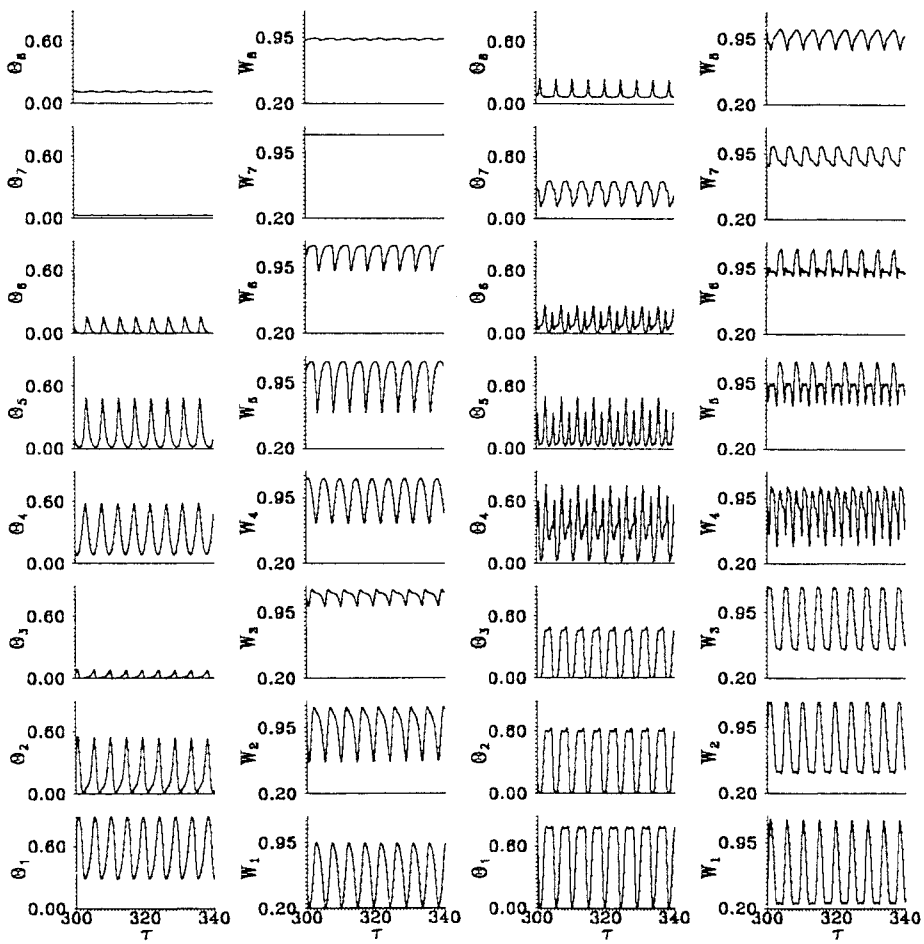

Fig. 10 Time histories of the axial velocity and temperature at Z = 1.963 and 3.329 at eight selected locations for Re_H = 3000 and Gr_H/Re_H^2 = 3.

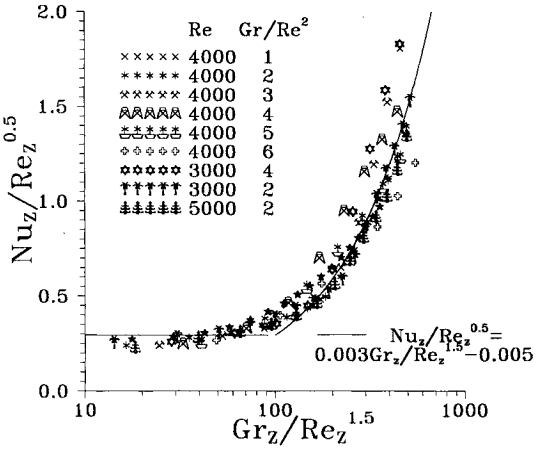

Fig. 11 Correlation for the spanwise-averaged Nusselt number with the mixed convection instability parameters for the data from the present prediction.

shows that the vortex flow patterns are very different with the same $Gr_Z/Re_Z^{1.5}$, but different Re_Z and Gr_Z. Therefore, the parameter is only suitable for characterizing the heat transfer data.

Within the range of $120 \leq Gr_H/Re_H^{1.5} \leq 500$, the minimum wavelength of the longitudinal rolls λ_{min} can be expressed by a simple correlation as

$$(\lambda_{min}/Z)(Gr_Z/Re_Z^{1.5})^{1/2} = 2\pi \tag{17}$$

Concluding Remarks

A transient three-dimensional numerical simulation was carried out in this study to investigate the temporal evolution of flow and thermal structures in a mixed convective vortex flow over an isothermal horizontal plate. The results were obtained for air with Re_Z up to 1.2×10^4, and Gr_Z up to 2.55×10^6. The major results are summarized below:

1) For $Gr_Z/Re_Z^{1.5} < 100$, two-dimensional laminar forced convection dominates and the flow quickly approaches steady state. The local Nusselt number monotonically decreases in the downstream direction.

2) In the range of $Gr_Z/Re_Z^{1.5}$, between 100–200, a three-dimensional vortex flow starts to form. Significant heat transfer enhancement is noted in this vortex flow regime. For $Gr_Z/Re_Z^{1.5}$ below 300, the vortex flow gradually reaches a steady state after the initial transient has died out.

3) The merging of the vortex rolls takes place for $Gr_Z/Re_Z^{1.5} > 400$ when $Gr_H/Re_H^2 = 6$. These larger vortex rolls are rather unstable. The vortices do not merge for $Gr_H/Re_H^2 = 3$. For $Gr_Z/Re_Z^{1.5} > 600$, the flow is also unstable even without vortex roll merging.

4) The parameter $Gr_Z/Re_Z^{1.5}$ is only suitable in characterizing the spanwise-average heat transfer coefficient.

During the course of this investigation, we realize that the number of nodes placed in each coordinate direction is not large enough to adequately resolve the steep velocity and temperature gradients in the thin layer of vortex flow on the bottom plate. It is also recognized that the employed step sizes in space and time are not small enough to directly capture the high-frequency small disturbances in the flow. These disturbances are nearly isotropic and rather dissipative. Thus, a subgrid modeling of certain type can be used to account for their influences on the flow. In view of the limited available computation capacity for this work, the multilevel multigrid scheme or other advanced schemes can also be used to improve the results in the future. Results for the mixed convective water flow on the horizontal plate are also of interest. Effects of the plate inclination can also be examined in the future.

Acknowledgments

The financial support of this study by the Engineering Division of the National Science Council of Taiwan through Contract NSC82-0404-E009-141 is greatly appreciated. The support of the present computation by the National Center for High-Performance Computing and by the Computer Center of the National Chiao Tung University, Taiwan, Republic of China, is also acknowledged.

References

[1]Aung, W., and Worku, G., "Developing Flow and Flow Reversal in a Vertical Channel with Asymmetric Wall Temperature," *Journal of Heat Transfer*, Vol. 108, No. 2, 1986, pp. 299–304.

[2]Mori, Y., "Buoyancy Effects in Forced Laminar Convection Flow over a Horizontal Flat Plate," *Journal of Heat Transfer*, Vol. 83, No. 4, 1961, pp. 479–482.

[3]Sparrow, E. M., and Minkowycz, W. J., "Buoyancy Effects on Horizontal Boundary-Layer Flow and Heat Transfer," *International Journal of Heat and Mass Transfer*, Vol. 5, No. 4, 1962, pp. 505–511.

[4]Hieber, C. A., "Mixed Convection Above a Heated Horizontal Surface," *International Journal of Heat and Mass Transfer*, Vol. 16, No. 4, 1973, pp. 769–785.

[5]Chen, T. S., Sparrow, E. M., and Mucoglu, A., "Mixed Convection in Boundary Layer Flow on a Horizontal Plate," *Journal of Heat Transfer*, Vol. 99, No. 1, 1977, pp. 66–71.

[6]Mucoglu, A., and Chen, T. S., "Mixed Convection on a Horizontal Plate with Uniform Surface Heat Flux," *Proceedings of the 6th International Heat Transfer Conference*, Vol. 1, Hemisphere, Washington, DC, 1978, pp. 85–90.

[7]Ramachandran, N., Armaly, B. F., and Chen, T. S., "Mixed Convection over a Horizontal Plate," *Journal of Heat Transfer*, Vol. 105, No. 2, 1983, pp. 420–423.

[8]Wu, R. S., and Cheng, K. C., "Thermal Instability of Blasius Flow Along Horizontal Plates," *International Journal of Heat and Mass Transfer*, Vol. 19, No. 8, 1976, pp. 907–913.

[9]Moutsoglou, A., Chen, T. S., and Cheng, K. C., "Vortex Instability of Mixed Convection Flow over a Horizontal Flat Plate," *Journal of Heat Transfer*, Vol. 103, No. 2, 1981, pp. 257–261.

[10]Yoo, J. Y., Park, P., Choi, C. K., and Ro, S. T., "An Analysis on the Thermal Instability of Forced Convection Flow over Isothermal Horizontal Flat Plate," *International Journal of Heat and Mass Transfer*, Vol. 30, No. 5, 1987, pp. 927–935.

[11]Lee, H. R., Chen, T. S., and Armaly, B. F., "Non-Parallel Thermal Instability of Forced Convection Flow over a Heated, Non-Isothermal Horizontal Flat Plate," *International Journal of Heat and Mass Transfer*, Vol. 33, No. 9, 1990, pp. 2019–2028.

[12]Lee, H. R., Chen, T. S., and Armaly, B. F., "Non-Parallel Vortex Instability of Natural Convection Flow over a Non-Isothermal Horizontal Flat Plate," *International Journal of Heat and Mass Transfer*, Vol. 34, No. 1, 1991, pp. 305–313.

[13]Lee, H. R., Chen, T. S., and Armaly, B. F., "Non-Parallel Thermal Instability of Natural Convection Flow on Non-Isothermal Inclined Flat Plates," *International Journal of Heat and Mass Transfer*, Vol. 35, No. 1, 1992, pp. 207–220.

[14]Lee, H. R., Chen, T. S., and Armaly, B. F., "Nonparallel Thermal Instability of Mixed Convection Flow on Non-Isothermal Horizontal and Inclined Flat Plates," *International Journal of Heat and Mass Transfer*, Vol. 35, No. 8, 1992, pp. 1913–1992.

[15]Chen, K., and Chen, M. M., "Thermal Instability of Forced Convection Boundary Layer," *Journal of Heat Transfer*, Vol. 106, No. 2, 1984, pp. 284–288.

[16]Gilpin, R. R., Imura, H., and Cheng, K. C., "Experiments on the Onset of Longitudinal Vortices in Horizontal Blasius Flow Heated from Below," *Journal of Heat Transfer*, Vol. 100, No. 1, 1978, pp. 71–77.

[17]Imura, H., Gilpin, R. R., and Cheng, K. C., "An Experimental Investigation of Heat Transfer and Buoyancy Induced Transition from Laminar Forced Convection to Turbulent Free Convection over a Horizontal Isothermally Heated Plate," *Journal of Heat Transfer*, Vol. 100, No. 3, 1978, pp. 429–434.

[18]Wang, X. A., "An Experimental Study of Mixed, Forced, and Free Convection Heat Transfer from a Horizontal Flat Plate to Air," *Journal of Heat Transfer*, Vol. 104, No. 1, 1982, pp. 139–144.

[19]Takimoto, A., Hayashi, Y., and Matsuda, O., "Thermal Instability of Blasius Flow over a Horizontal Plate," *Heat Transfer—Jap-*

anese Research, Vol. 12, No. 1, 1983, pp. 19–33.

[20]Moharreri, S., Armaly, B. F., and Chen, T. S., "Measurements in the Transitional Vortex Flow Regime of Mixed Convection Above a Horizontal Heated Plate," *Journal of Heat Transfer*, Vol. 110, No. 2, 1988, pp. 358–365.

[21]Cheng, K. C., and Kim, Y. W., "Flow Visualization Studies on Vortex Instability of Natural Convection Flow over Horizontal and Slightly Inclined Constant Temperature Plates," *Journal of Heat Transfer*, Vol. 110, No. 3, 1988, pp. 608–615.

[22]Chorin, A. J., "Numerical Solution of the Navier-Stokes Equations," *Mathematics of Computation*, Vol. 22, No. 104, 1968, pp. 745–762.

[23]Kawamura, T., Takami, H., and Kuwahara, K., "New Higher-Order Upwind Scheme for Incompressible Navier-Stokes Equations," *Proceeding of the 9th International Conference on Numerical Methods in Fluid Dynamics*, edited by Soubbaramayer and Bonjot, Springer-Verlag, Berlin, 1985, pp. 176–179.

[24]Hirsch, C., "Numerical Computation of Internal and External Flow," Vol. 1, Wiley, New York, 1989, pp. 176–179.

[25]Anderson, D. A., Tannehill, J. C., and Pletcher, R. H., "Computational Fluid Mechanics and Heat Transfer," Hemisphere, Washington, DC, 1984, pp. 71–77.

[26]Cheng, K. C., Obata, T., and Gilpin, R. R., "Buoyancy Effects on Forced Convection Heat Transfer in the Transition Regime of Horizontal Boundary Layer Heated from Below," *Journal of Heat Transfer*, Vol. 110, No. 3, 1988, pp. 596–603.